Desalination and Water Treatment
www.deswater.com

doi: 10.1080/19443994.2015.1056841

57 (2016) 13334–13346
June

Taylor & Francis
Taylor & Francis Group

Adsorption of direct green 26 onto fix 3500 treated sawdust: equilibrium, kinetic and isotherms

A. Hashem[a,b,*], F. Ahmad[c], Sayed M. Badawy[d,e]

[a]*Faculty of Science and Arts at Shaqra, Shaqra University, Shaqra, Saudi Arabia, email: alihashem2000@yahoo.com*
[b]*Textile Research Devision, National Research Center, Dokki, Cairo, Egypt*
[c]*Faculty of Engineering, Textile Department, Mehran University, Jamshoro, Pakistan*
[d]*Faculty of Science, Chemistry Department, Aljouf University, Sakaka, Saudi Arabia*
[e]*Faculty of Medicine, National Center for Clinical and Environmental Toxicology, Cairo University, Cairo, Egypt*

Received 12 February 2015; Accepted 19 May 2015

ABSTRACT

Cationized sawdust (CSD) was prepared by the reaction of sawdust (SD) with cationizing agent. Three levels of CSD having different nitrogen content were prepared. The CSD samples were characterized by estimation of nitrogen content. The feasibility of CSD to remove C.I. Direct Green (DG 26) dye from aqueous solutions was examined. The impacts of several operating parameters such as adsorbent dose, adsorption time, and adsorbate concentration on the adsorption capacity were investigated. The CSD was effectively used in adsorption of DG 26 dye from aqueous solutions. In order to determine the best fit isotherm, the experimental equilibrium data were analyzed using eight adsorption isotherm models including Langmuir, Freundlich, Temkin, and Dubinin–Radushkevich (two parameter models), Redlich–Peterson, Toth, Sips and Khan (three parameter models) using non-linear regression technique. Tempkin and Sips isotherms were found to best represent the data for DG 26 dye than other isotherms. The kinetics of adsorption of DG 26 dye have been discussed using six kinetic models, i.e., the pseudo-first-order model, the pseudo-second-order model, Batacharia–Venkobachar, the Elovich equation, the intraparticle diffusion model, and Bangham equation. The removal of DG 26 dye onto CSD particles could be well described by the pseudo–second-order model. CSD dye was found to be inexpensive and effective adsorbent for removal of DG 26 dye from aqueous solutions.

Keywords: Sawdust; Direct green 26; Adsorption isotherm; Cationized sawdust; Wastewater treatment

1. Introduction

The effluents from the dyestuff manufacturing and textile industries, in particular, are highly colored with a large amount of suspended organic solids and considered as important sources of water pollution. Dyes have become one of the main sources of severe water pollution as a result of the rapid development of the textile industries. The release of the colorant effluent has triggered a major concern on the human health as well as marine lives [1].

Many of the dyes are stable to light and oxidation, as well as resistant to aerobic degradation. Therefore,

---

*Corresponding author.

conventional methods such as chemical precipitation, chemical coagulation, chemical oxidation, and biological treatment methods are ineffective for their removal [2,3]. In a country where economy plays a very big role, it is better to find low-cost adsorbents to be used in this field. Therefore, there is a need to search for an effective adsorbent for economical wastewater treatment. The adsorption process is one of the efficient methods to remove the dyes from effluent [4]. The process of adsorption has an edge over the other methods due to its clean process and complete removal of dyes even from dilute solutions.

Direct dyes possess good affinity to cellulosic fibers and they are widely used due to their low cost, excellent color range, and good light fastness [5]. Many of them are highly toxic and carcinogenic [6].

Sawdust (SD) is an abundant by-product of the wood industry and easily available at the countryside at zero or negligible price. It contains various organic compounds (lignin, cellulose, and hemicellulose) with polyphenolic groups useful for binding direct dyes [7]. Most of the studies showed that native or modified SD is highly efficient for the removal of direct dyes [8–11].

The attention of our previous work aimed to utilize modified cellulose [12], and cellulosic fabric wastes [13] as well as SD treated glycidyltrimethyl ammonium acetate for the removal of anionic dyes from aqueous solutions. The latter was found to exhibit a much better adsorption capacity toward anionic dyes than native SD [14]. The adsorption capacity of direct dyes onto native or modified SD in the literature is still small and the present work aims to increase the adsorption capacity of SD toward direct dyes. In comparison between the cationized sawdust (CSD) adsorbent in the present study and other adsorbents in similar studies [15–17] toward adsorption of direct dyes, the CSD is good adsorbent for direct green 26 (DG 26).

The present article reports the feasibility CSD as a low-cost adsorbent for the removal of DG 26 dye from aqueous solutions. In this study, the experimental parameters for the adsorption of DG 26 from aqueous solutions under different equilibrium conditions were investigated in a batch study. The kinetics of adsorption of DG 26 on the adsorbent has been studied using different models. Five error functions were used to treat the equilibrium data using non-linear optimization techniques for evaluating the fit of the isotherm equations in order to optimize the design of adsorption system for the removal of DG 26 dye utilizing CSD.

2. Experimental

2.1. Materials

Swedish wood SD was kindly supplied from one of wood manufacturing companies, Cairo, Egypt. The proximate analyses of SD are shown in Table 1.

2.2. Reagents

EDTA, acetic acid, NaOH, and ethanol were of laboratory grade and used without further purification. DG 26 dye was kindly supplied from Ismadye Company, Egypt, and was not purified prior to use. The structure of DG 26 and its molecular weight are shown in Table 2. Commercial CA (Fix 3500) was supplied from Dyestuffs, Pigments Manufacturer, Taiwan. The scientific name of this reagent is polyamine and its chemical structure is unknown.

2.3. Methods

2.3.1. Preparation of adsorbent (CSD)

Three levels of CSD with various nitrogen contents were prepared by keeping other reaction conditions constant and varying the amount of CA as shown in Table 3. The reaction was carried out as follows: SD (4 g) with mesh size 200–300 μm was mixed well by spatula with 15 ml of 2 N NaOH solution in a 100 ml Erlenmeyer flask. The required amount of CA was added to the flask. The resulting reaction mixture was maintained in a thermostatic water bath at 60˚C for 2 h. After completion of the reaction, the resulting mixture was neutralized by treatment with acidified ethanol, the reaction product was washed several times with distilled water and finally dried at 105˚C for 2 h.

2.3.2. Adsorption studies

Aqueous solutions of DG 26 were prepared by dissolving the dye in distilled water to the required

Table 1
The chemical characteristics of sawdust

Analysis	Content %
Ash	3
Hemicellulose	15
Lignin	31
Cellulose	51

Table 2
The chemical structure and molecular weight of DG 26

Color index	Chemical structure	Molecular weight
DG 26	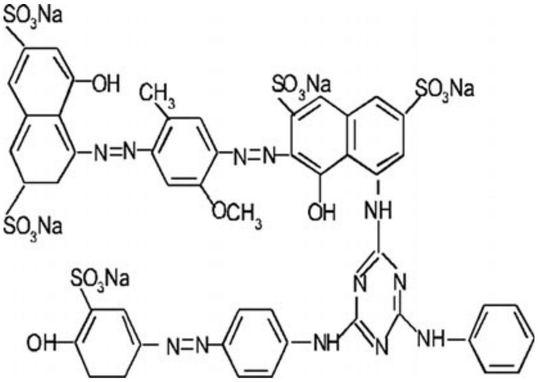	1333.07

concentrations without pH adjustment. In an equilibrium experiment, a certain amount of aminated SD particles and 100 ml of an aqueous dye solution were placed in a 125 ml glass stoppered flask and stirred for specific time using a shaking water bath operated at 200 rpm at 30˚C. The samples were withdrawn from the shaker, and the dye solution was separated from the adsorbent by centrifugation. Dye concentration in the supernatant solution was measured with a Shimadzu UV/Visible Spectrophotometer. The amount of DG 26 adsorbed, q_e (mg/g), and per cent removal of DG 26 on CSD were calculated according to the following equations:

$$q_e = \frac{(C_o - C_e) \cdot V(l)}{W} \tag{1}$$

$$\text{Percent removal} = \frac{C_o - C_e}{C_o} \times 100\% \tag{2}$$

where C_o and C_e are the initial and final concentrations of DG 26, mg, V is the volume of dye solution (l), W is the weight of CSD (g). All experiments were carried out in duplicate and the mean values of q_e were reported.

2.4. Analyses

2.4.1. Determination of nitrogen content

The nitrogen content of SD and CSD samples was determined using the micro-Kjeldahl method [18]. Accurately, 0.2 g of the sample was introduced in Kjeldahl digestion tube. 5 g K_2SO_4 + 0.5 g $CuSO_4$ in 1 ml conc. H_2SO_4were added to the sample. The sample was digested for 1 h. 20 ml of deionized water was added to the sample after allowing it to cool. After adding 25 ml of 40% NaOH, the sample was then distilled in Kjeldahl apparatus and the ammonia liberated was collected in 1 N boric acid and titrated with 0.03 N HCl. The nitrogen content of SD or CSD was calculated as follows:

$$N\% = \frac{V_{\text{HCl}} \cdot N_{\text{HCl}} \cdot 0.014}{W(\text{g})} \cdot 100 \tag{3}$$

where, V is the volume of HCl consumed; N is the normality of standard HCl; W is the weight of the sample (g).

2.5. Error analysis

In the single-component isotherm studies, the optimization procedure requires an error function to be

Table 3
The characteristics of CDS samples

Code sample	CA* (ml)	NaOH (mmole)	N %	Adsorption capacity (mg/g)
Unmodified SD	0	30	0.1	9.3
A	1	30	0.55	16.7
B	2	30	0.95	22.1
C	4	30	2.1	35.4

*The chemical structure of CA is unknown.

defined to evaluate the fit of the isotherm to the experimental equilibrium data. The common error functions for determining the optimum isotherm parameters were average relative error (ARE), sum of the squares of the errors (ERRSQ), hybrid fractional error function (HYBRID), Marquardt's per cent standard deviation (MPSD), and sum of absolute errors (EABS) [19]. In the present study, all error functions were used to determine the best fit in isotherm model as:

2.5.1. *Average relative error*

$$\mathrm{ARE} = \sum_{i=1}^{n} \left| \frac{(q_e)_{\mathrm{exp.}} - (q_e)_{\mathrm{calc.}}}{(q_e)_{\mathrm{exp.}}} \right|_i \tag{4}$$

2.5.2. *Average percentage error (APE)*

$$\mathrm{APE}\% = \frac{\sum_{i=1}^{N} \left| [((q_e)_{\mathrm{exp.}} - (q_e)_{\mathrm{calc.}})/q_{\mathrm{exp.}}] \right|}{N} \times 100 \tag{5}$$

2.5.3. *The sum of the squares of the error*

$$\mathrm{ERRSQ} = \sum_{i=1}^{n} \left[(q_e)_{\mathrm{calc.}} - (q_e)_{\mathrm{exp.}} \right]^2 \tag{6}$$

2.5.4. *Hybrid fraction error function*

$$\mathrm{Hybrid} = \frac{100}{n-p} \sum_{i=1}^{n} \left[\frac{((q_e)_{\mathrm{exp.}} - (q_e)_{\mathrm{calc.}})^2}{(q_e)_{\mathrm{exp.}}} \right]_i \tag{7}$$

2.5.5. *Marquardt's per cent standard deviation*

$$MPSD = 100\sqrt{\frac{1}{n-p} \sum_{i=1}^{n} \left[\frac{((q_e)_{\mathrm{exp.}} - (q_e)_{\mathrm{calc.}})}{(q_e)_{\mathrm{exp.}}} \right]^2} \tag{8}$$

2.5.6. *The sum of absolute error*

$$\mathrm{EABS} = \sum_{i=1}^{n} \left| (q_e)_{\mathrm{exp.}} - (q_e)_{\mathrm{calc.}} \right|_i \tag{9}$$

3. Results and discussion

3.1. *Factors affecting adsorption of DG 26 onto CSD*

3.1.1. *Effect of adsorbent concentration (adsorbent dose)*

The effect of adsorbent concentration on both adsorption capacity and per cent removal of DG26 on CSD are shown in Fig. 1. It is clear from this figure that the per cent removal of DG 26 increases from 31.42 to 99.4% by increasing the concentration of adsorbent from 0.3 to 4 g/l. The increase in per cent removal of DG 26 with increasing adsorbent concentration could be attributed to the greater availability of the exchangeable sites of the adsorbent. On the other hand, the adsorption capacity (q_e), or the amount of DG 26 adsorbed per unit mass of adsorbent (mg/g), decreases by increasing the concentration of adsorbent (Fig. 1). The decrease in adsorption capacity with increasing the adsorbent concentration is mainly due to overlapping of the adsorption sites as a result of overcrowding of the adsorbent particles and is also due to the competition among DG 26 for the surface sites [20].

3.1.2. *Effect of contact time*

Fig. 2 shows the effect of contact time on the adsorption capacity, q_e (mg/g) of DG 26 onto CSD at 30˚C using adsorbate concentration of 100 mg/l at fixed adsorbent concentration. Equilibrium adsorption was established after 120 min within the concentration range studied. It is further observed that the adsorption curve is smooth and continuous, which indicate

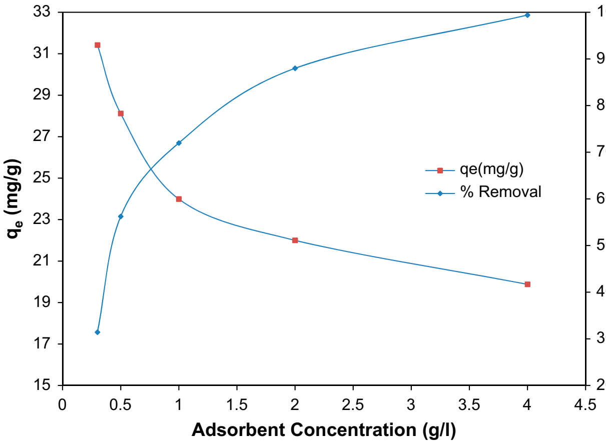

Fig. 1. Effect of adsorbent concentration on adsorption capacity of DG 26 at 30˚C. Reaction Conditions: DG 26 Concentration, 100 mg/l; Agitation Time, 3 h; Adsorption Temperature, 30˚C.

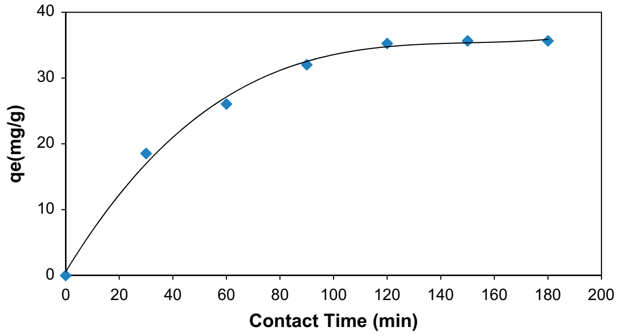

Fig. 2. Effect of contact time on adsorption capacity of DG 26 onto CSD at 30˚C. Reaction Conditions: Adsorbent Conc. 0.3 g/l; DG 26, 100 mg/l; Adsorption Temperature, 30˚C.

the possibility of the formation of monolayer coverage of DG 26 onto CSD. This datum is important because equilibrium time is one of the parameters for economical wastewater treatment.

3.1.2.1. *Kinetics of adsorption.* Six kinetic models, viz. pseudo-first-order, Bhattacharya–Venkobachar, Pseudo-second-order, Bangham, intraparticle diffusion, and Elovich models were used to investigate the adsorption process of DG 26 on CSD.

3.1.2.2. *Pseudo-first-order model.* The pseudo-first-order equation [21] is:

$$\frac{dq_t}{dt} = k_1(q_e - q_t) \tag{10}$$

where q_t is the amount of adsorbate adsorbed at time t (mg/g), q_e is the adsorption capacity at equilibrium (mg/g), k is the pseudo-first-order rate constant (min^{-1}), and t is the contact time (min). The integration of Eq. (4) with the initial condition, $q_t = 0$ at $t = 0$, the following equation is obtained:

$$\log(q_e - q_t) = \log q_e - \frac{k \cdot t}{2.303} \tag{11}$$

In order to obtain the rate constants, the straight line plot of log ($q_e - q_t$) against t for DG 26 onto CSD have been tested. The intercept of this plot should give log q_e. However, if the intercept does not equal to q_e, the reaction is not likely to be first order even if this plot has high correlation coefficient (R^2) with the experimental data [22]. For the data obtained in the present study, the plots of log ($q_e - q_t$) vs. t as required by Eq. (5) for the adsorption of DG 26 at initial concentrations of 100 mg/l by CSD (Fig. 3) gave correlation coefficients, R^2, which had low values. This indicates that the adsorption of DG 26 onto CSD is not acceptable for this model.

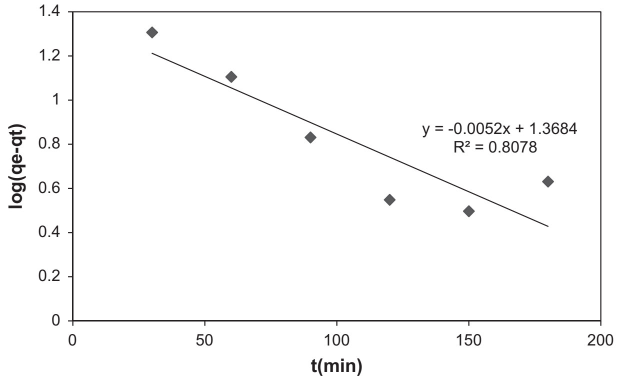

Fig. 3. Pseudo-first-order reaction of DG 26 onto CSD at 30˚C.

3.1.2.3. *Bhattacharya–Venkobachar model.* The Bhattacharya–Venkobachar [23] equation is:

$$\log[1 - U_t] = -\left(\frac{k}{2.303}\right)t \text{ where } U_t = [(C_o - C_t)/(C_o - C_e)] \tag{12}$$

where C_o, C_t, and C_e are the concentration of DG 26 (mg/l) at time zero, time, t, and at equilibrium time and k is the first-order rate constant (min^{-1}) for adsorption of DG 26 onto CSD. The value of R^2 for the concentration of 100 mg/l (Fig. 4) is very low. This indicates that the adsorption of DG 26 onto CSD is not acceptable for this model.

3.1.2.4. *Pseudo-second-order model.* The pseudo-second-order model [22] is represented as:

$$\frac{dq_t}{dt} = k_2(q_e - q_t)^2 \tag{13}$$

where k_2 is the pseudo-second-order rate constant (g/mg min). Integrating Eq. (13) with the initial condition, $q_t = 0$ at $t = 0$, the following equation is obtained:

$$\frac{t}{q_t} = \frac{1}{(k_2 \cdot q_e^2)} + \frac{t}{q_{e_t}} \tag{14}$$

where k_2 is the pseudo-second-order adsorption rate constant. This equation predicts that if the system follows pseudo-second-order kinetics, the plot of t/q_e vs.

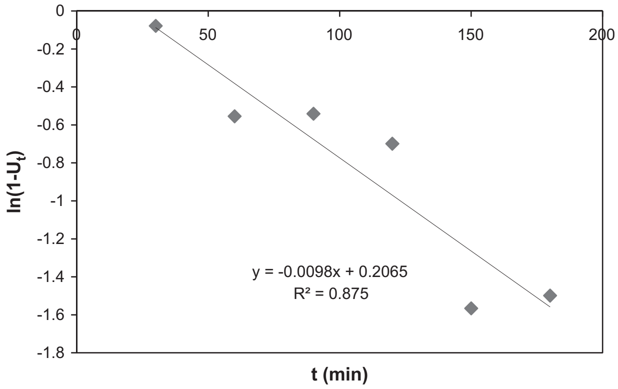

Fig. 4. Bhattacharya–Venkobachar model of DG 26 onto CSD at 30˚C.

t should be linear. Plotting the experimental data obtained for the adsorption of DG 26 at initial concentration of 100 mg/l onto CSD according to the relationship given in Eq. (14) gave linear plots with correlation coefficient, R^2, of 0.9918 for DG 26as shown in Fig. 5 and listed in Table 4, thereby indicating the applicability of the pseudo-second-order kinetic equation to the experimental data. The first-order and pseudo-second-order models cannot identify the diffusion mechanism, and the kinetic results were then subjected to analyze by the intra-particle diffusion model.

3.1.2.5. Bangham model. Bangham's model [24] was employed for applicability of adsorption of DG 26 onto CSD, whether the adsorption process is diffusion controlled.

$$\log\left(\frac{C_o}{C_o - q \cdot m}\right) = \log\left(\frac{k_o m}{2.303V}\right) + \alpha \log t \tag{15}$$

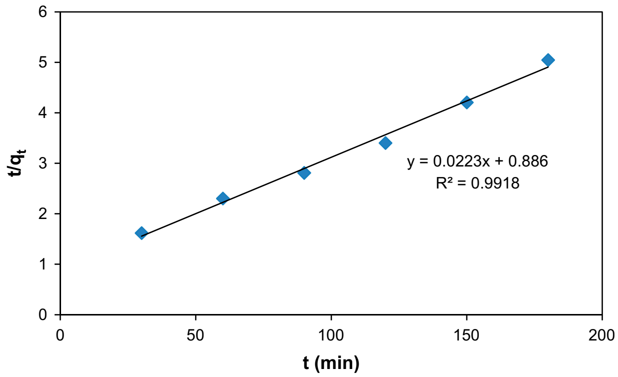

Fig. 5. Pseudo-second-order reaction of DG 26 onto CSD at 30˚C.

Table 4
Kinetic parameters for adsorption of DG 26 onto CSD at 30˚C

Models	Parameters	Values
k_1	Pseudo-first-order	
R^2		
k_1	Bhattacharya–Venkobachar	
R^2		
k_1	Pseudo-second-order	5.61×10^{-4}
q_e (exp.)		35.66
q_e (calc.)		44.84
R^2		0.9918
K_o	Bangham's equation	1.33
α		0.2358
R^2		0.99
K_P	Intra-particle diffusion	0.1871
C		13.94
R^2		0.9714
α	Elovich equation	2.27
β		0.097
R^2		0.9714

where C_o is initial concentration of adsorbate (mg/l), V is volume of dye solution (ml), m is weight of adsorbent used per liter of solution (g/l), q is the amount of adsorbate retained at time t (mg/g), α (<1), and k_0 are constants.

The double logarithmic plot, according to Eq. (15), yield satisfactory linear curves for the adsorption of DG 26 by CSD. The correlation coefficient value, R^2 (Fig. 6 and Table 4) was 0.9434 for the concentration of 100 mg/g. This indicates that the adsorption of DG 26 onto CSD is acceptable for this model and shows that the diffusion of adsorbate into the pores of the adsorbent was the rate-controlling step [25].

3.1.2.6. Intra-particle diffusion. The intra-particle diffusion model [26] can be expressed by the following equation:

$$q_t = k_P \cdot t^{\frac{1}{2}} + C \tag{16}$$

where k_p is the intra-particle diffusion rate constant (mg/g^1 min$^{-1/2}$) and q_t is the amount of solute adsorbed per unit mass of adsorbent. The data of solid phase metal concentration against time t at the initial concentration of 100 mg/l of DG 26 were further processed for testing the rate of diffusion in the adsorption process. Adsorption process incorporates the transport of adsorbate from the bulk solution to the interior surface of the pores in CSD. The rate parameter for intra-particle diffusion, k_p for the DG 26on CSD is measured according to Eq. (16). The plots of q_t vs. $t^{1/2}$ for the DG 26 concentration of 100 mg/l is shown in Fig. 7.

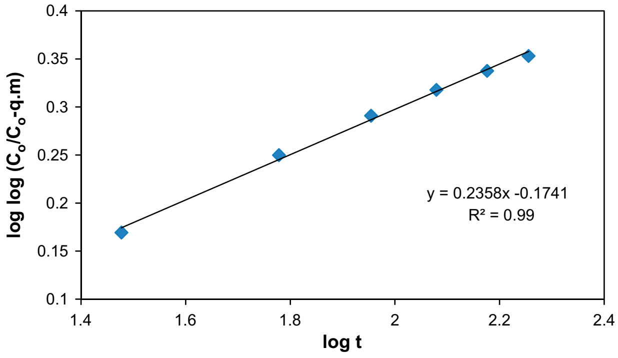

Fig. 6. Bangham model of DG 26 onto CSD at 30˚C.

Different previous studied indicated that the plots of q_t vs. $t^{1/2}$ were multi-linear two or more steps govern the adsorption process [27–29]. The plot is curved at the initial portion followed by linear portion and plateau. The initial curved portion is attributed to the bulk diffusion and the linear portion to the intra-particle diffusion, while the plateau corresponding to equilibrium. The deviation of straight lines from the origin (Fig. 8) may be because of the difference between the rate of mass transfer in the initial and final stages of adsorption. Further, such deviation of straight line from the origin indicates that the pore diffusion is not the rate-controlling step [30]. The values of k_p (mg/g min) obtained from the slope of the straight line (Fig. 8) are listed in Table 4. The value of R^2 for the plot is listed also in Table 4. The values of intercept C (Table 4) give an idea about the boundary layer thickness, i.e., the larger the intercept, the greater the boundary layer effect [31]. This value indicates that the adsorption of DG 26 onto CS is inacceptable for intra-particle diffusion mechanism.

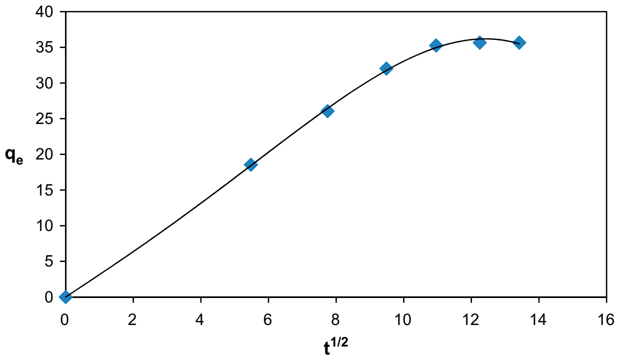

Fig. 7. Intra-particle diffusion model of DG 26 onto CSD at 30˚C.

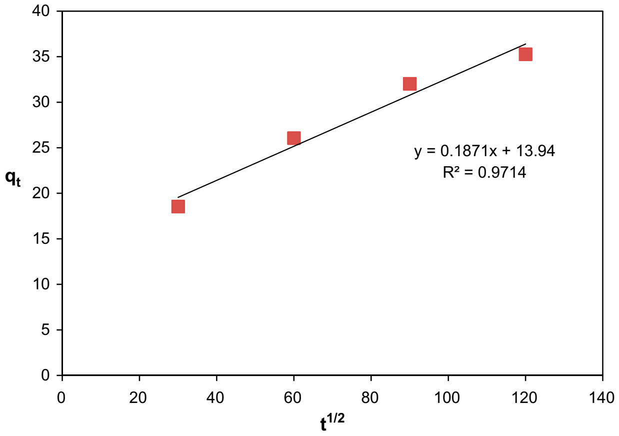

Fig. 8. Test of intra-particle diffusion model of DG 26 onto CSD at 30˚C.

3.1.2.7. Elovich equation. The Elovich model equation [32] is generally expressed as:

$$\frac{\mathrm{d}q_t}{\mathrm{d}t} = \alpha \exp.(-\beta.q_t) \tag{17}$$

where α is the initial adsorption rate (mg/g min) and β is the adsorption constant (g/mg) during the experiment. To simplify the Elovich equation, Chien and Clayton [32] assumed $\alpha\beta \gg 1$ and by applying the boundary conditions $q = 0$ at $t = 0$ and $q_t = q_t$ at $t = t$, Eq. (17) become:

$$q_t = \frac{1}{\beta}\ln(\alpha\beta) + \frac{1}{\beta}\ln(t) \tag{18}$$

If DG 26 adsorption onto CSD fits the Elovih model, a plot of q_e vs. $\ln t$ should yield a linear relationship with a slope of $1/\beta$ and an intercept of$1/\beta \ln(\alpha\beta)$. Fig. 9 shows a plot of linearization form of Elovich model at the DG 26 concentration of 100 mg/l. The slope and intercept of the plot of q_t vs. $\ln t$ was used to determine the constant β and the initial adsorption rate α. The correlation coefficient value, R^2 for the plot is listed in Table 4. The correlation coefficient for the Elovich kinetic model obtained at the DG 26 concentration of 100 mg/l was over 0.95. This indicates that the adsorption of DG 26 onto CSD is acceptable for this model.

3.1.2.8. Mechanism of adsorption of DG 26 on CSD. Prediction and identifying the mechanism of the adsorption process are important factors to be considered for proper design purposes. The mechanism of dye uptake may be attributed to: (a) intra-particle diffusion

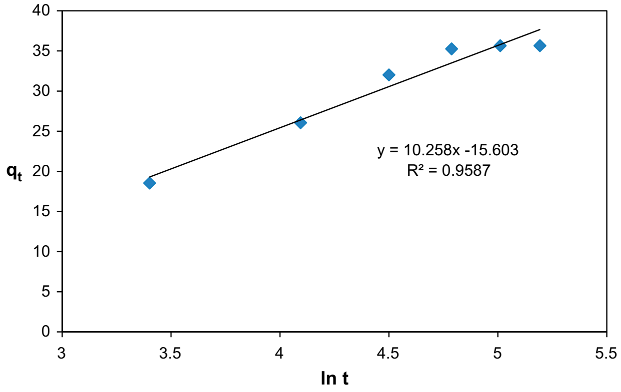

Fig. 9. Elovich model of DG 26 onto CSD at 30˚C.

mechanism as mentioned before, and (b) the chemical reaction between positive charge of cationic groups on the surface of CSD and the negative charge in DG 26 forming a cation-exchange reaction due to high cation-exchange capacity of the CSD as well as physical adsorption of dye molecules on the adsorbent surface.

3.1.3. Effect of adsorbate concentration

3.1.3.1. Adsorption isotherm. Adsorption isotherms describe how adsorbates interacting with adsorbents are critical in optimizing the use of adsorbents. The amount of adsorbate per unit mass of adsorbent at equilibrium, q_e (mg/g) and the adsorbate equilibrium concentration, C_e (mg/l) allows plotting the adsorption isotherm, q_e vs. C_e (Fig. 10) at 30˚C. The adsorption capacity values for DR 26 obtained was found to be 35.7 mg/g. In comparison with other adsorbents reported in the literature for adsorption of DR 26, the CSD had a good affinity for removal of DR 26 as shown in Table 5 [15–17].

Mathematical models can be used to describe and characterize the adsorption process. The eight most common isotherms for describing solid–liquid sorption systems are the Langmuir, the Freundlich, Temkin, Dubinin (two parameter isotherms), Redlich–Peterson isotherms, Toth, Sips, Khan and Hill (three parameter isotherms). Therefore, in order to investigate the adsorption capacity of DG 26 onto CSD, the experimental data were fitted to these equilibrium models.

3.1.3.2. Two parameter isotherms.

(1) The Langmuir model

Langmuir equation [33] was applied for adsorption equilibrium of DG 26 by CSD. The assumption of this model is based on the maximum adsorption corresponding to a saturated monolayer of adsorbate molecules on the adsorbent surface and the energy of adsorption is constant as well as there is no transmigration of adsorbate in the plane surface. The nonlinear form of Langmuir isotherm is given by the following equation:

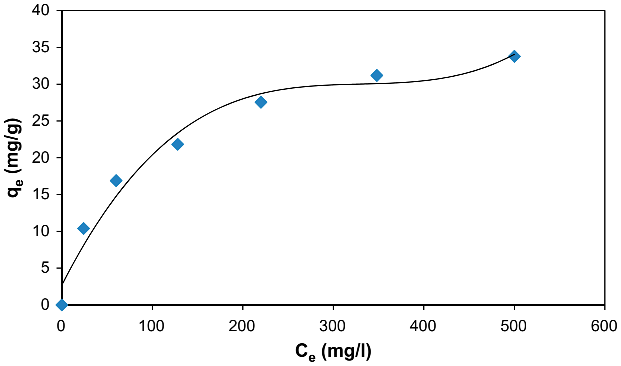

Fig. 10. Equilibrium adsorption isotherm of DG 26 adsorption onto CSD at 30˚C. Reaction Conditions: Adsorbent Conc., 0.3 g/l; Agitation Time, 120 min; Adsorption Temperature, 30˚C.

$$q_e = \frac{k_L \cdot C_e}{1 + a_L \cdot C_e} \tag{19}$$

where, a_L is Langmuir isotherm constant (l/mg), K_L is the Langmuir constant (l/g) and K_L/a_L represents the adsorption capacity, q_{max} (mg/g).

(2) The Freundlich model

The Freundlich model [34] is a special case applied to non-ideal adsorption on heterogeneous surfaces and also to multilayer adsorption, suggesting that binding sites are not equivalent and/or independent. This model is described by Eq. (20) as follows:

$$q_e = K_F \cdot C_e^{1/n} \tag{20}$$

where q_e is the equilibrium concentration of DG 26 on CSD adsorbent (mg/g), C_e the equilibrium concentration of DG 26 in dye solution (mg/l), and K_F (mg/g) and n are the Freundlich constants characteristic of the system, indicators of adsorption capacity and adsorption intensity, respectively.

(3) The Tempkin model

The Temkin isotherm [35] has been used in the following form:

Table 5
Comparison of sorption capacities of various adsorbents for DG 26

Adsorbents	Adsorption capacity (mg/g)	References
Squid pen	4.8	[15]
Deprotenized squid pen	37.0	[15]
Andonta shell	11.3	[16]
Sepia pen	58.0	[16]
Beach wood sawdust	2.78	[17]
Cationized sawdust	35.7	This study
Natural sawdust	9.3	This study

$$q_e = \frac{RT}{b_T}\ln(A_T C_e) \tag{21}$$

where R is the universal gas constant (8.31441 $\mathrm{J^{-1}\,mol^{-1}\,K^{-1}}$), T is the absolute temperature (K), A_T is the Temkin isotherm constant (g/mg), and b_T is Temkin constant.

(4) Dubinin–Radushkevich isotherm

This isotherm is generally expressed as follows [36]:

$$q_e = q_D \cdot \exp.\left(-B_D\left[RT\ln\left(1+\frac{1}{C_e}\right)\right]\right)^2 \tag{22}$$

Dubinin–Radushkevich have reported that the characteristic sorption curve is related to the porous structure of the sorbent. The constant, B_D is related to the mean free energy of sorption per mole of the sorbate as it is transferred to the surface of the solid from infinite distance in the solution and this energy can be computed using the following relationship by Hasany and Chaudhary [37] as:

$$E = \frac{1}{\sqrt{2B_D}} \tag{23}$$

3.1.3.3. *Three parameter isotherms.*

(1) Redlich–Peterson isotherm

Redlich–Peterson model is used as a compromise between Langmuir and Freundlich models, which can be written as [38]:

$$q_e = \frac{A \cdot C_e}{1 + B \cdot C_e^g} \tag{24}$$

where KRP (L/g), αRP (L/mmol), and β are Redlich–Peterson constants. The value of β lies between 0 and 1, $C_e^g$is the equilibrium liquid-phase concentration of the adsorbate (mg/l), and q_e is the equilibrium adsorbate loading onto the adsorbent (mg/g).

(2) Toth isotherm

Toth isotherm model [39] is useful in describing heterogeneous adsorption systems, which satisfies both low and high-end boundary of the concentration [40]. It can be represented by the following equation:

$$q_e = \frac{k_t \cdot C_e}{(a_t + C_e)^{1/t}} \tag{25}$$

where k_t, a_t, and t are the Toth isotherm constants.

(3) Sips isotherm

Sips isotherm [41] is a combined form of Langmuir and Freundlich expressions deduced for predicting the heterogeneous adsorption systems and circumventing the limitation of the rising adsorbate concentration associated with Freundlich isotherm model. Sips model can be represented by the following equation:

$$q_e = \frac{k_s \cdot C_{es}^B}{1 + a_s . C_{es}^B} \tag{26}$$

where k_s is the Sips model isotherm constant (L/g), a_s the Sips model constant (L/mg), and B_s the Sips model exponent. At low sorbate concentrations, it effectively reduces to the Freundlich isotherm and thus does not obey Henry's law.

(4) Khan isotherm

Khan isotherm [42] is a generalized model suggested for the pure solutions, with b_K and a_K are

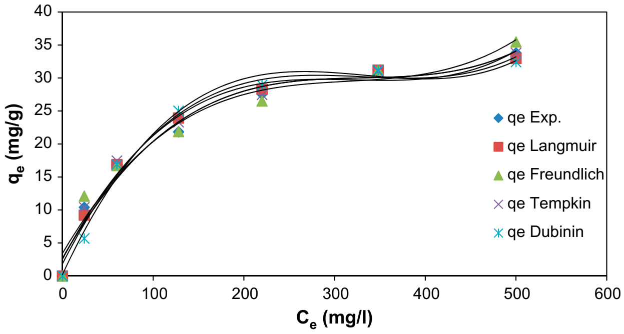

Fig. 11. Comparison of two parameter models with experimental data at 30˚C.

devoted to the model constant and model exponent. Khan isotherm model can be represented by:

$$q_e = \frac{q_K \cdot b_K \cdot C_e}{(1 + b_K \cdot C_e)^{a_K}} \tag{27}$$

where b_K is the Khan model constant, a_K the Khan model exponent, and q_K is the maximum uptake (mg/g).

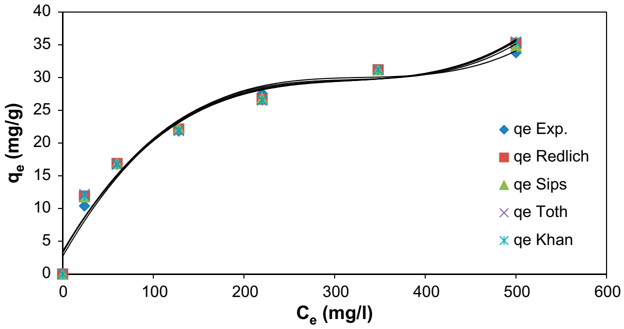

Fig. 12. Comparison of three parameter models with experimental data at 30˚C.

3.2. Error analysis and non-linear regression method

In nonlinear regression method, the validity of widely used isotherm models to the experimental data was examined by trial-and-error using the solver add-in with Microsoft Excel. The R^2 value is used to minimize the error distribution between the experimental equilibrium data and the predicted isotherms

The fitting presentation of two and three parameter models are shown in Figs. 11 and 12 as well as the

Table 6
Constants and error analysis of two parameter models for adsorption of DG 26 onto CSD at 30˚C

Isotherm model	Parameter	Value	Error analysis	Value
Langmuir	a_L	0.013392	ARE	0.261664
			APE%	4.36107
	k_L	0.507476	EABS	4.853864
			ERRSQ	7.002804178
	R^2	0.987	Hybrid	9.372364
			MPSD	0.942296
Freundlich	$1/n$	0.354196	ARE	0.2625567
			APE%	4.375946
	k_F	3.925871	EABS	4.624346
			ERRSQ	6.796441499
	R^2	0.9625	Hybrid	10.03949
			MPSD	0.952468
Tempkin	A_T	0.160643	ARE	0.109391281
			APE%	1.823188
	b_T	3.226111	EABS	2.300598
			ERRSQ	2.489146395
	R^2	0.9749	Hybrid	2.939873692
			MPSD	0.936423572
Dubinin–Radushkevich	q_D	35.47339	ARE	0.690133
			APE%	11.50221
	B_D	0.9021678	EABS	10.65889
			ERRSQ	36.14360088
	R^2	0.9913	Hybrid	68.1693
			MPSD	0.967955

Table 7
Constants and error analysis of three parameter models for adsorption of DG 26 onto CSD at 30˚C

Isotherm model	Parameter	Value	Error analysis	Value
Redlich–Peterson	A	4.376162	ARE	0.232382
			APE%	3.873027
	B	0.911169	EABS	4.108512
			ERRSQ	5.130892
	G	0.676717	Hybrid	7.690230788
			MPSD	0.950012292
	R^2	0.9646		
Toth	k_t	4.011966	ARE	0.266287
			APE%	4.438112
	a_t	0.090949	EABS	4.607884
			ERRSQ	6.872671
	$1/t$	0.649482	Hybrid	10.60390374
			MPSD	0.953263
	R^2	0.9749		
Sips	K_s	3.078928	ARE	0.208688
			APE%	3.478132
	a_s	0.03233	EABS	3.542168
			ERRSQ	3.593645
	B_s	0.463543	Hybrid	5.965622915
			MPSD	0.948112
	R^2	0.9663		
Khan	q_K	2.037966	ARE	0.2574942
			APE%	4.29157
	a_K	0.6447771	EABS	4.596818
			ERRSQ	6.635122942
	b_K	6.231578	Hybrid	9.490784096
			MPSD	0.951715
	R^2	0.9633		

constants and error analysis of two and three parameter models are given in Tables 6 and 7. Among two and three parameter models, the highest R^2 value and lowest ARE, APE %, EABS, ERRSQ, MPSD, and Hybrid values were observed with Tempkin (two parameter) followed by Sips (three parameter) models indicating the better fit than the rest of isotherm models.

4. Conclusions

SD has been utilized as adsorbent material for the removal of DG 26 from contaminated water after treatment with commercial CA, Fix 3500 in alkaline medium to form CSD. The CSD sample was characterized by estimating the nitrogen content. The ability of CSD to adsorb DG 26 was investigated by using batch adsorption procedure. The data of the adsorption isotherm were tested by the Langmuir, Freundlich and Temkin, Dubinin (two parameter models), Redlich–Peterson, Toth, Sips, and Khan (three parameter models) using non-linear regression technique. The best fitting model was firstly evaluated using six different error functions. The examination of all these error estimation methods showed that the Tempkin and Sips models provide the best fit for experimental data than other isotherms. The kinetics of adsorption of DG 26 have been discussed using six kinetic models, i.e., the pseudo-first-order model, the pseudo-second-order model, Batacharia, the Elovich equation, the intraparticle diffusion model and Bangham equation. The adsorption of DG 26onto CSD could be well described by the pseudo-second-order kinetic model.

References

[1] W.S. Wan Ngah, L.C. Teong, M.A.K.M. Hanafiah, Adsorption of dyes and heavy metal ions by chitosan composites: A review, Carbohydr. Polym. 83 (2011) 1446–1456.

[2] G. McKay, Adsorption of dyestuffs from aqueous solutions with activated carbon I: Equilibrium and batch contact-time studies, J. Chem. Technol. Biotechnol. 32 (1982) 759–772.

[3] S. Nethaji, A. Sivasamy, G. Thennarasu, S. Saravanan, Adsorption of Malachite Green dye onto activated carbon derived from Borassus aethiopum flower biomass, J. Hazard. Mater. 181 (2010) 271–280.

[4] K.G. Sreejalekshmi, K.A. Krishnan, T.S. Anirudhan, Adsorption of Pb(II) and Pb(II)-citric acid on sawdust activated carbon: Kinetic and equilibrium isotherm studies, J. Hazard. Mater. 161 (2009) 1506–1513.

[5] J. Zhang, Y. Li, C. Zhang, Y. Jing, Adsorption of malachite green from aqueous solution onto carbon prepared from Arundo donax root, J. Hazard. Mater. 150 (2008) 774–782.

[6] M.T. Yagub, T.K. Sen, S. Afroze, H.M. Ang, Dye and its removal from aqueous solution by adsorption: A review, Adv. Colloid Interface Sci. 209 (2014) 172–184.

[7] Z.M. Magriotis, S.S. Vieira, A.A. Saczk, N.A.V. Santos, N.R. Stradiotto, Removal of dyes by lignocellulose adsorbents originating from biodiesel production, J. Environ. Chem. Eng. 2 (2014) 2199–2210.

[8] A. Hebeish, M. Ramadan, E. Abdel-Halim, A. Abo-Okeil, An effective adsorbent based on sawdust for removal of direct dye from aqueous solutions, Clean Technol. Environ. Policy 13 (2011) 713–718.

[9] V. Dulman, S.M. Cucu-Man, Sorption of some textile dyes by beech wood sawdust, J. Hazard. Mater. 162 (2009) 1457–1464.

[10] R. Ansari, B. Seyghali, A. Mohammad-khah, M.A. Zanjanchi, Highly efficient adsorption of anionic dyes from aqueous solutions using sawdust modified by cationic surfactant of acetyl trimethyl ammonium bromide, J. Surfactants. Deterg. 15 (2012) 557–565.

[11] D. Sidiras, F. Batzias, E. Schroeder, R. Ranjan, M. Tsapatsis, Dye adsorption on autohydrolyzed pine sawdust in batch and fixed-bed systems, Chem. Eng. J. 171 (2011) 883–896.

[12] A. Hashem, R.M. El-shishtawy, Preparation and characterization of cationized cellulose for the removal of anionic dyes, Adsorp. Sci. Technol. 19 (2001) 197–210.

[13] H.H. Sokker, E.S. Abdel-Halim, A.S. Aly, A. Hashem, Cellulosic fabric wastes grafted with DMAEMA for the removal of direct dyes, Adsorp. Sci. Technol. 22 (2004) 679–691.

[14] A. Hashem, A.A. Aly, A.S. Aly, Preparation and utilization of cationized sawdust, Polym. Plast. Technol. Eng. 45 (2006) 395–401.

[15] S.A. Figueiredo, J.M. Loureiro, R.A. Boaventura, Natural waste materials containing chitin as adsorbents for textile dyestuffs: Batch and continuous studies, Water Res. 39 (2005) 4142–4152.

[16] S.A. Figueiredo, R.A. Boaventura, J.M. Loureiro, Color removal with natural adsorbents: modeling, simulation and experimental, Sep. Purif. Technol. 20 (2000) 129–141.

[17] S. Izadyar, M. Rahimi, Use of beech wood sawdust for adsorption of textile dyes, Pak. J. Biol. Sci. 10 (2007) 287–293.

[18] A. Vogel, Textbook of quantitative inorganic analysis including elementary instrumental analysis, Longman Group Ltd, London, 1972.

[19] S.C. Tsai, K.W. Juang, Comparison of linear and non-linear forms of isotherm models for strontium sorption on a sodium bentonite, J. Radioanal. Nucl. Chem. 243 (2000) 741–746.

[20] A. HashemH.H. SokkerE.S. Abdel HalimA. Gamal, γ-Induced graft copolymerization onto cellulosic fabric waste for cationic dye removal, Adsorp.Sci. Technol. 23 (2005) 455–465.

[21] H.C. Trivedi, V.M. Patel, R.D. Patel, Adsorption of cellulose triacetate on calcium silicate, Eur. Polym. J. 9 (1973) 525–531.

[22] Y.S. Ho, G. McKeay, The kinetics of sorption of divalent metal ions onto sphagnum moss peat, Water Res. 34 (2000) 735–742.

[23] A.K. Bhattacharya, C. Venkobachar, Removal of cadmium (II) by low cost adsorbents, J. Environ. Eng. 110 (1984) 110–122.

[24] E. Tutem, R. Apak, C.F. Unal, Adsorptive removal of chlorophenols from water by bituminous shale, Water Res. 32 (1998) 2315–2324.

[25] F.C. Wu, R.L. Tseng, R.S. Juang, Initial behavior of intraparticle diffusion model used in the description of adsorption kinetics, Chem. Eng. J. 153 (2009) 1–8.

[26] W.J. Weber, J.C. Morris, Advances in water pollution research. Proc 1st Int. Conf on Water Pollut. Res. 2 (1962) 231–266.

[27] H.K. Boparai, M. Joseph, D.M. O'Carroll, Kinetics and thermodynamics of cadmium ion removal by adsorption onto nano zerovalent iron particles, J. Hazard. Mater. 186 (2011) 458–465.

[28] E.I. Unuabonah, K.O. Adebowale, B.I. Olu-Owolabi, Kinetic and thermodynamic studies of the adsorption of lead (II) ions onto phosphate-modified kaolinite clay, J. Hazard. Mater. 144 (2007) 386–395.

[29] F.C. Wu, R.L. Tseng, R.S. Juang, Initial behavior of intraparticle diffusion model used in the description of adsorption kinetics, Chem. Eng. J. 153 (2009) 1–8.

[30] V.J.P. Poots, G. McKay, J. Healy, Removal of basic dye from effluent using wood as an adsorbent, J. Water. Pollut. Control Fed. 50 (1978) 926–935.

[31] K. Nagarethinam, M.S. Mariappan, Kinetics and mechanism of removal of methylene blue by adsorption on various carbons-a comparative study, Dyes Pigm. 51 (2001) 25–40.

[32] S.H. Chien, W.R. Clayton, Application of elovich equation to the kinetics of phosphate release and sorption in soils, Soil Sci. Soc. Am. J. 44 (1980) 265–268.

[33] I. Langmuir, The constitution and fundamental properties of solids and liquids. part I. solids, J. Am. Chem. Soc. 38 (1916) 2221–2295.

[34] H.M.F. Freundlich, Over the adsorption in solution, J. Phys. Chem. 57 (1906) 1100–1107.

[35] M.I. Tempkin, V. Pyzhev, Kinetics of ammonia synthesis on promoted iron catalysts, Acta Physiochim URSS 12 (1940) 217–222.

[36] M.M. Dubinin, Modern state of the theory of volume filling of micropore adsorbents during adsorption of gases and steams on carbon adsorbents, Zeitschrift für Physikalische Chemie 39 (1965) 1305–1317.

[37] S.M. Hasany, M.H. Chaudhary, Sorption potential of Hare River sand for the removal of antimony from acidic aqueous solution, Appl. Radiat. Isot. 47 (1996) 467–471.

[38] O.J.D.L. Redlich, D.L. Peterson, A useful adsorption isotherm, J. Phys. Chem. 63 (1959) 1024–1026.

[39] J. Toth, State equations of the solid gas interface layer, Acta Chem. Acad. Hung. 69 (1971) 311–317.

[40] K. Vijayaraghavan, T.V.N. Padmesh, K. Palanivelu, M. Velan, Biosorption of nickel(II) ions onto Sargassum wightii: Application of two-parameter and three-parameter isotherm models, J. Hazard. Mater. 133 (2006) 304–308.

[41] R. Sips, On the Structure of a Catalyst Surface, J. Chem. Phys. 16 (1948) 490–495.

[42] A.R. Khan, R. Ataullah, A. Al-Haddad, Equilibrium adsorption studies of some aromatic pollutants from dilute aqueous solutions on activated carbon at different temperatures, J. Colloid Interface Sci. 194 (1997) 154–165.